Supplementary Information

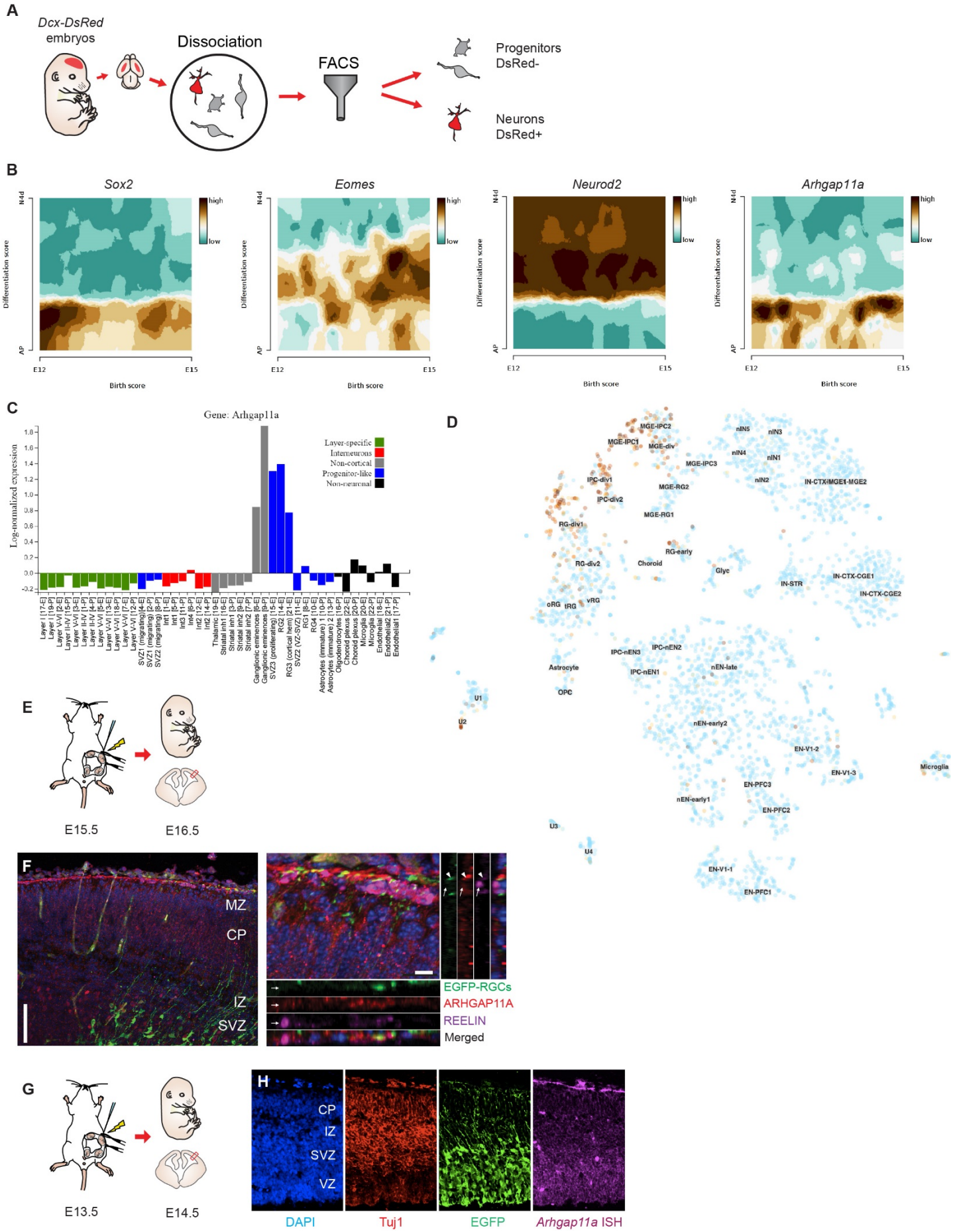

Figure S1. *Arhgap11a* expression is restricted to neural progenitors in mice and humans,

Related to Figure 1.

(A) Cartoon showing the strategy used to perform qPCR analysis of mRNA levels in sorted embryonic cortical cells in Figure B.

(B-D) Published single-cell RNA-sequencing analyses confirm *Arhgap11a* expression is restricted to neural progenitors in mice from E12 to E15 (B): (Telley et al., 2019), in mice at E14.5 and P0 (C): (Loo et al., 2019), and in human fetal cortices from peak neurogenesis stages (D) (Nowakowski et al., 2017).

(E,F) Double immunofluorescence targeting ARHGAP11A and REELIN proteins shows that ARHGAP11A is not expressed in Reelin+ Cajal Retzius neurons. (F) arrowheads point to EGFP+ radial glia basal endfoot containing ARHGAP11A protein, arrows point to REELIN+ Cajal Retzius neurons devoid of ARHGAP11A immunofluorescence signal.

(G,H) *In situ* hybridization coupled with immunofluorescence in E14.5 EGFP-electroporated brains shows strong enrichment of *Arhgap11a* mRNA (purple) in EGFP+ basal endfeet (green)and not in Tuj1+ neurons (red).

FACS: fluorescence-activated cell sorting, ISH: in situ hybridization, EGFP: enhanced green fluorescent protein. Scale bars: F: left panel: 100 μm, right panel: 10 μm.

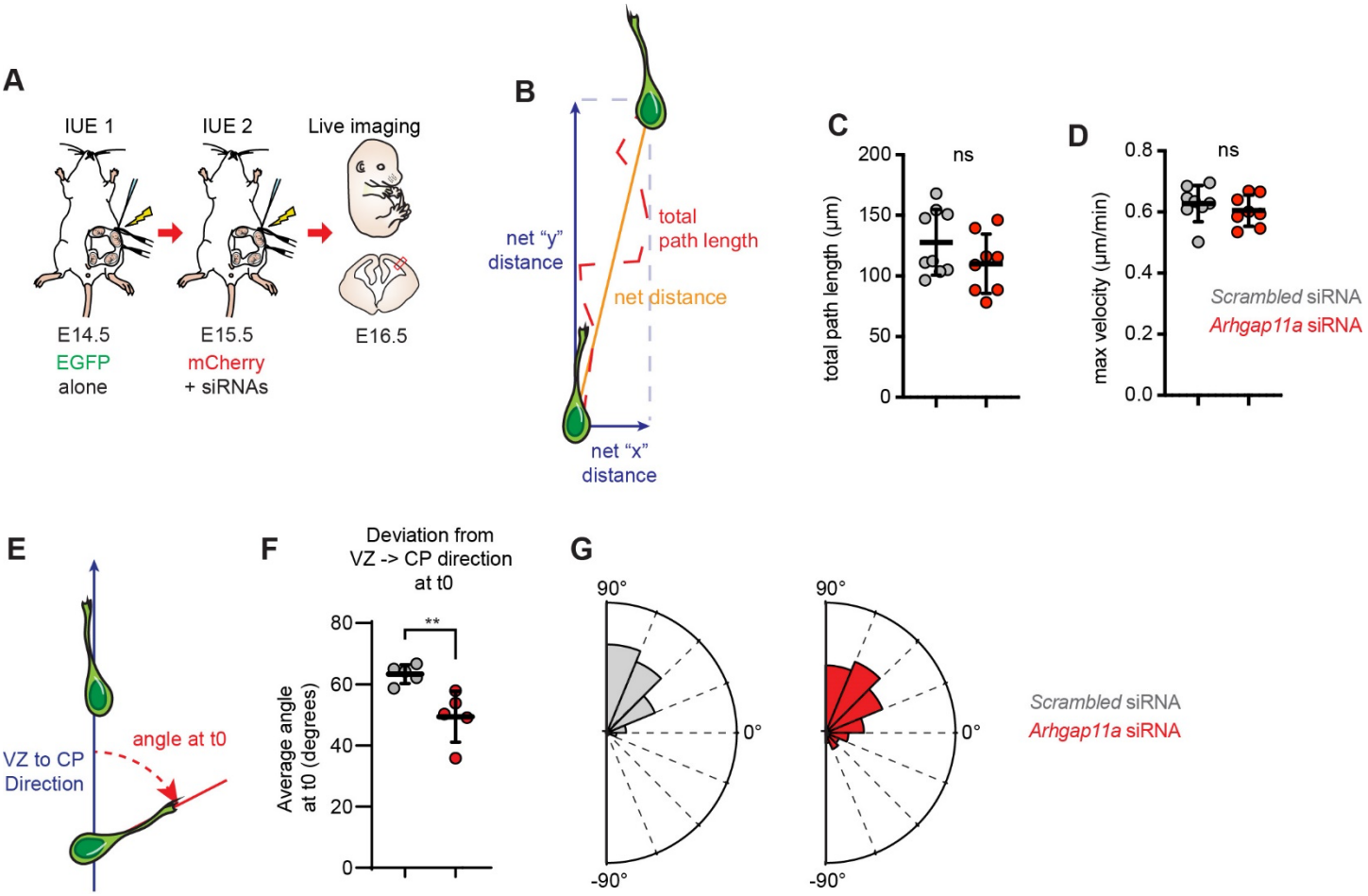

Figure S2. Neuronal migration parameters unaffected by depletion of *Arhgap11a* in RGCs, Related to Figure 2.

(A) Schematic overview of experiments to test the impact of *Arhgap11a* depletion in RGCs on neuronal migration.

(B) Neuronal migration parameters analyzed.

(C,D) Quantification of neuronal migration parameters, reflecting no defect in total path length nor max velocity following depletion of *Arhgap11a* in RGCs. (Scrambled and *Arhgap11a*: n=8 brains from 2 independent experiments, unpaired t-tests)

(E-G) Quantification of neurons orientation at t0 of the live imaging experiment in the SVZ-IZ following depletion of *Arhgap11a*. (Scrambled and *Arhgap11a*: n=10 brains from 2 independent experiments, 20-40 neurons per brain, unpaired t-tests).

IUE: *in utero* electroporation, siRNA: small interfering RNA, ns: non-significant.

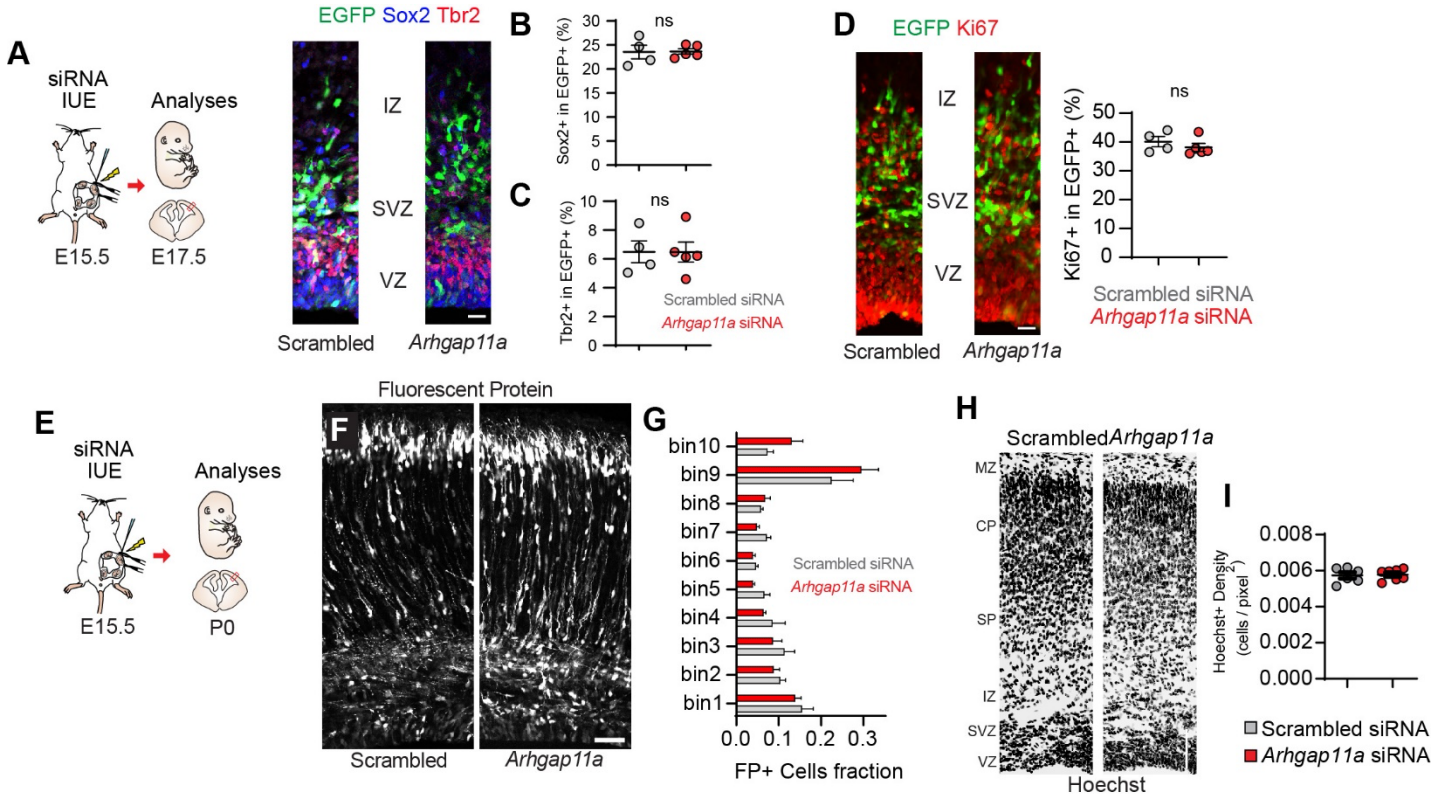

Figure S3. *Arhgap11a* depletion does not impact neural progenitor proliferation and numbers, Related to Figure 2.

(A) Schematic overview of experiments to test the impact of *Arhgap11a* depletion in RGCs progenitor proliferation and numbers.

(A,D) Representative images of regions analyzed at E17.5.

(B,C,D) Quantification of Sox2 (B), Tbr2 (C) and Ki67 (D) following *Arhgap11a* depletion. Note there is no defect in the number of neural progenitor subtypes and proliferation. (Scrambled: n=4 brains from 3 independent experiments, *Arhgap11a*: n=5 brains from 3 independent experiments, unpaired t-tests)

(E) Schematic overview of experiments to test the cell autonomous impact of *Arhgap11a* depletion on neuron positioning at P0.

(F) Representative images of regions analyzed at P0.

(G) Quantification of electroporated cell distribution at P0. (Scrambled: n= 3 brains from 2 independent experiments, *Arhgap11a:* n= 4 brains from 2 independent experiments, two-way ANOVA).

(H,I) Acute depletion of *Arhgap11a* at E15.5 in RGCs does not impact nuclei density in the cerebral cortex at P0. (Scrambled: n=6 brains from 3 IUE'd brains; Arhgap11a: n=7 brains from 3 IUE'd brains).

IUE: *in utero* electroporation, siRNA: small interfering RNA, FP: fluorescent protein, ns: non-significant, VZ: ventricular zone, SVZ : subventricular zone, IZ: intermediate zone. Scale bars

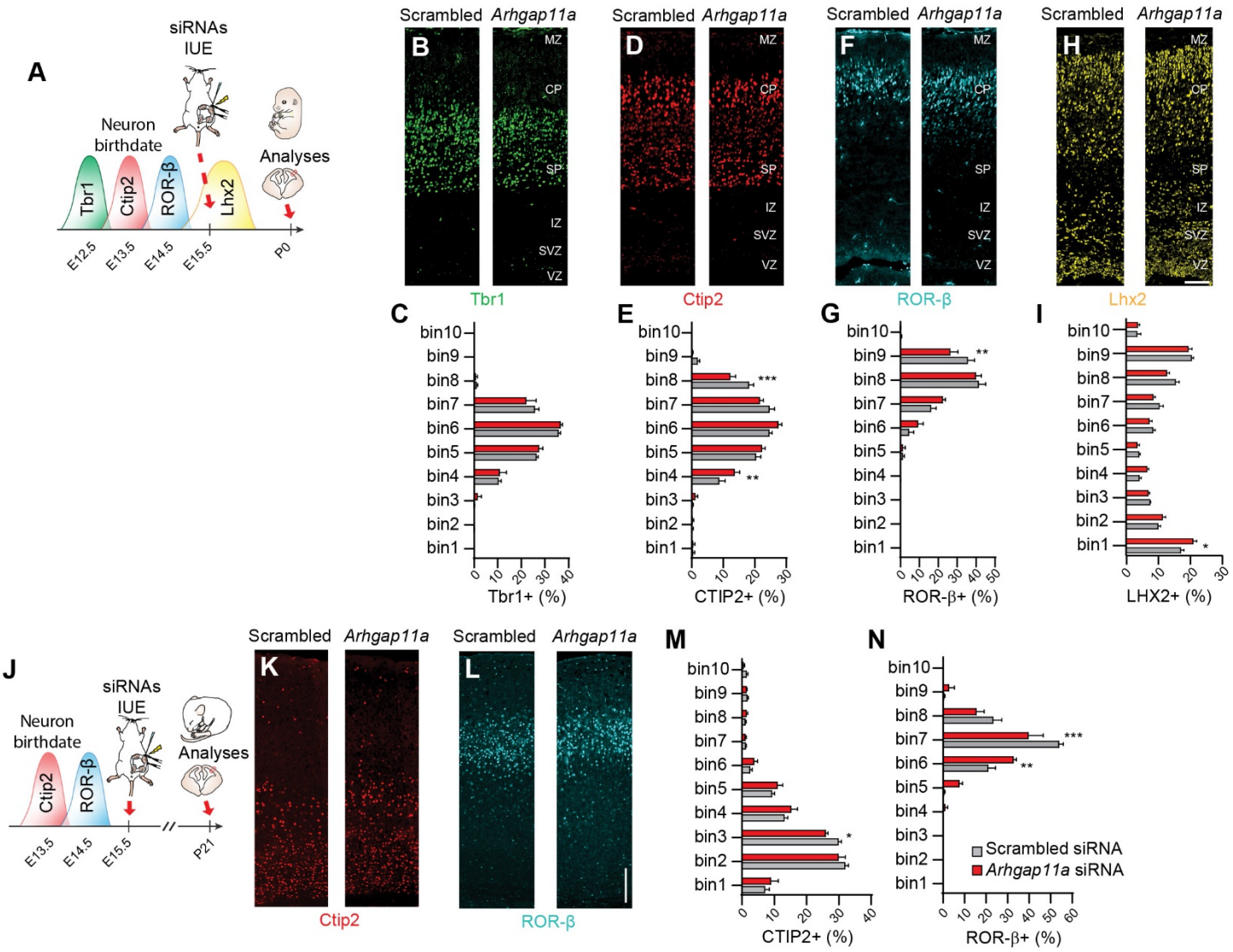

Figure S4. ARHGAP11A non-cell autonomously controls laminar architecture, Related to Figure 2.

(A) Schematic overview of the experiments in (B-I) which test the impact of acute *Arhgap11a* depletion at E15.5 on neuron positioning at P0. Waves of peak generation of excitatory neuronal subtypes generated prior to electroporation are represented.

(B,D,F,H) Representative images showing immunofluorescence of Tbr1 (green, B) Ctip2 (red, D), RorB (cyan, F) or Lhx2 (yellow, H) in P0 brains IUE'd with either scrambled or *Arhgap11a* siRNAs at E15.5.

(C,E,G,I) Acute depletion of *Arhgap11a* at E15.5 in RGCs has no impact on the distribution of early-born Tbr1+ neurons (C), but causes fewer later-born Ctip2+ (E), RorB+ (G) and Lhx2+ (I) neurons in the upper layers in the cerebral cortex at P0. (Scrambled: n=5-6 brains from 3 independent experiments, *Arhgap11a*: n=6-7 brains from 3 independent experiments. 2-way ANOVA with Bonferroni post-tests).

(J) Schematic overview of the experiments in (J-N) which test the impact of acute *Arhgap11a* depletion at E15.5 on neuron positioning at P21.

(K-N) Acute *Arhgap11a* depletion in RGCs at E15.5 causes fewer Ctip2+ (M) and Ror-B+ (N) neurons in bin3 and bins 7, respectively, at P21. (Scrambled: n=7 brains from 3 independent experiments, *Arhgap11a*: n=4 brains from 3 independent experiments. 2-way ANOVA with Bonferroni post-tests).

siRNAs: small interfering RNAs, IUE: *in utero* electroporation. VZ: ventricular zone, SVZ : subventricular zone, CP: cortical plate, IZ: intermediate zone. *: p-value<0.05, **: p-value<0.01. ***: p-value<0.001. Scale bars: B-E: 200 µm, K,L: 100 µm.

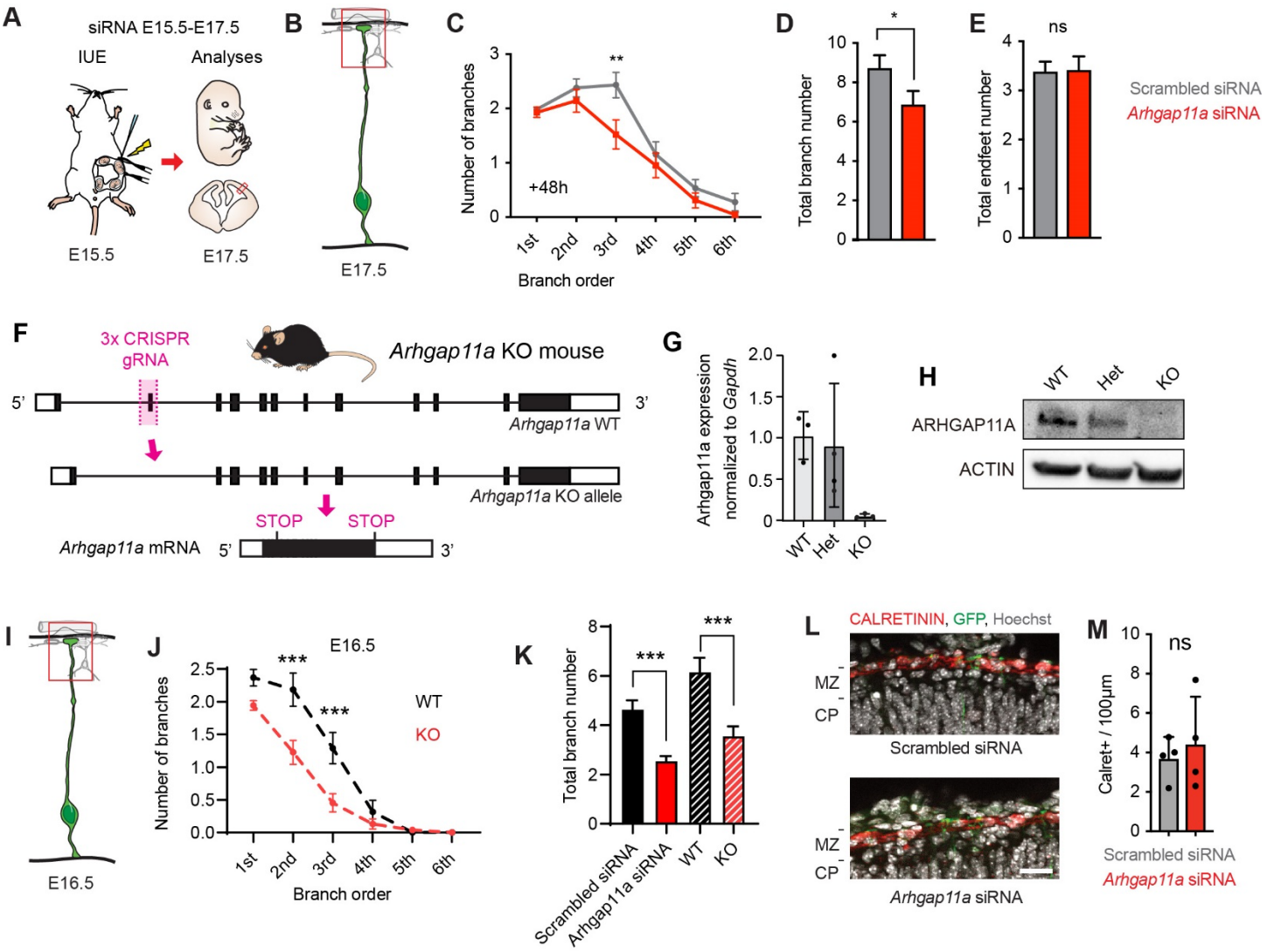

Figure S5. Effect of *Arhgap11a* knockdown in RGCs upon cells of the MZ, Related to Figure 3.

(A, B) Schematic overview of experiments in (C-E) to quantify the impact of acute *Arhgap11a* depletion on basal process complexity two days after electroporation. Brains were electroporated with GLAST::EGFP-CAXX to label RGCs. (Scrambled: n=58 processes from 5 brains, *Arhgap11a:* n=48 processes from 4 brains, two-way ANOVA, Sidak post-hoc analyses to compare individual branch orders)

(C, D) Reduction of RGC basal process complexity persists two days after introduction of *Arhgap11a* siRNAs.

(E) Endfoot number per RGC is not affected by depletion of *Arhgap11a* (D). (Scrambled: n=58 cells from 5 brains, 2 independent experiments, *Arhgap11a:* n=43 cells from 4 brains, 2 independent experiments, C,D: unpaired t-tests)

(F) Cartoon depicting the approach use to generate Arhgap11a KO mice.

(G, H) RT-PCR analyses (G) and Western blot (H) confirm loss of ARHGAP11A expression in *Arhgap11a* germline KO mice.

(I-K) Analyses of RGC basal process branching in the MZ of *Arhgap11a* KO E16.5 cortices shows defects similar to those observed after acute knockdown of *Arhgap11a* by siRNA treatments at E15.5 (WT: n=40

process from 3 brains, KO: n=53 process from 4 brains, two-way ANOVA, Sidak post-hoc analyses to compare individual branch orders).

(L,M) A one day knockdown of *Arhgap11a* in RGCs (E) has no impact on the number of CALRETININ+ cells (presumed Cajal Retzius neurons) lining the basement membrane. (Scrambled: n=4 brains from 3 independent experiments, *Arhgap11a:* n=4 brains from 3 independent experiments, unpaired t-test) *, non-specific signal from vasculature.

IUE: *in utero* electroporation, siRNA: small interfering RNA, *: p-value<0.05, *: p-value<0.01. ns: non-significant. Scale bar: L: 25 µm. Graphs show average values +/- SEM.

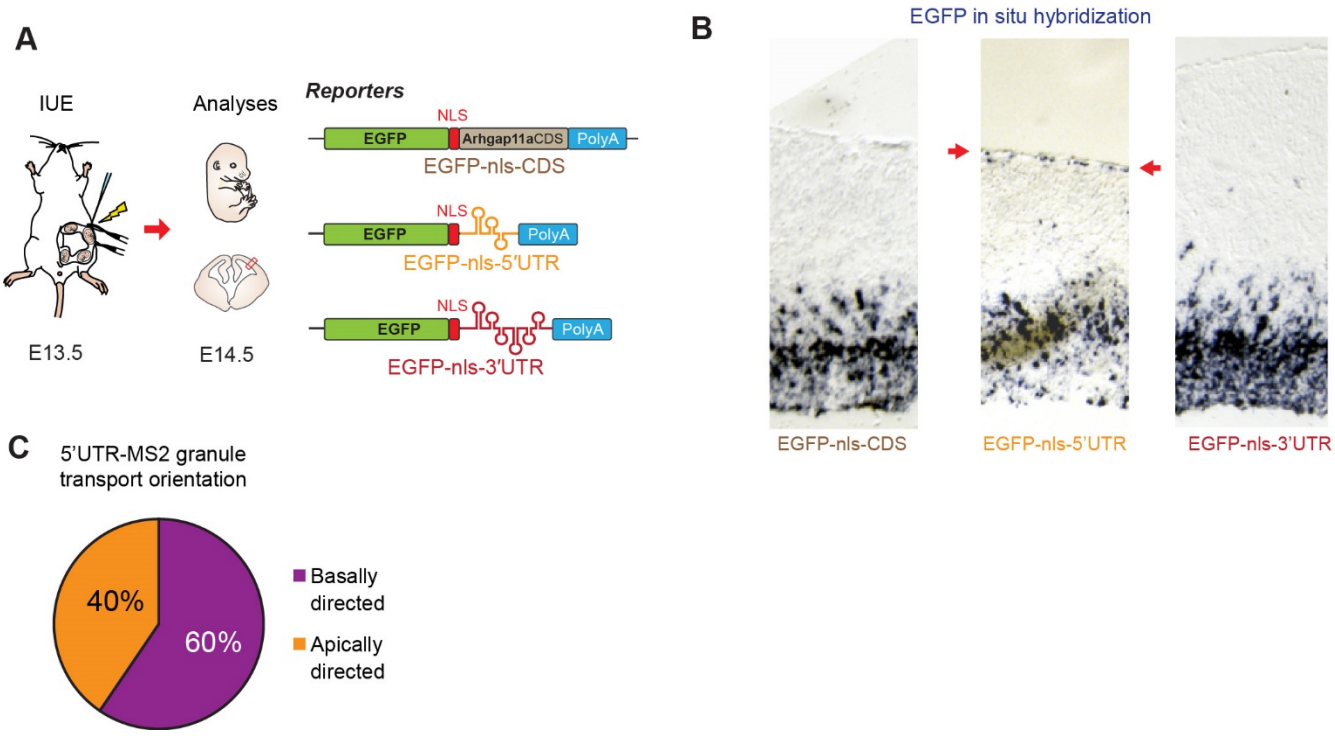

Figure S6. Localization of *Arhgap11a* mRNA to RGC basal endfeet and processes relies on a 5′UTR element,

Related to Figure 5.

(A) Strategy used to uncover the endfoot localization sequence in *Arhgap11a* mRNA.

(B) *In situ* hybridization against *EGFP* (purple) in E14.5 brains. Note EGFP-nls mRNA reporters localize to the pia only when they contain the *Arhgap11a* 5′UTR (red arrows denote enrichment in the basal endfeet region). This shows that *Arhgap11a* mRNA endfoot localization sequence resides in its 5′UTR.

(C) Orientation of 5′UTR -MS2 granule transport in RGC basal processes analyzed in Figure 5D-J.

IUE: *in utero* electroporation, CDS: coding sequence, UTR: untranslated region, nls: nuclear localization signal.

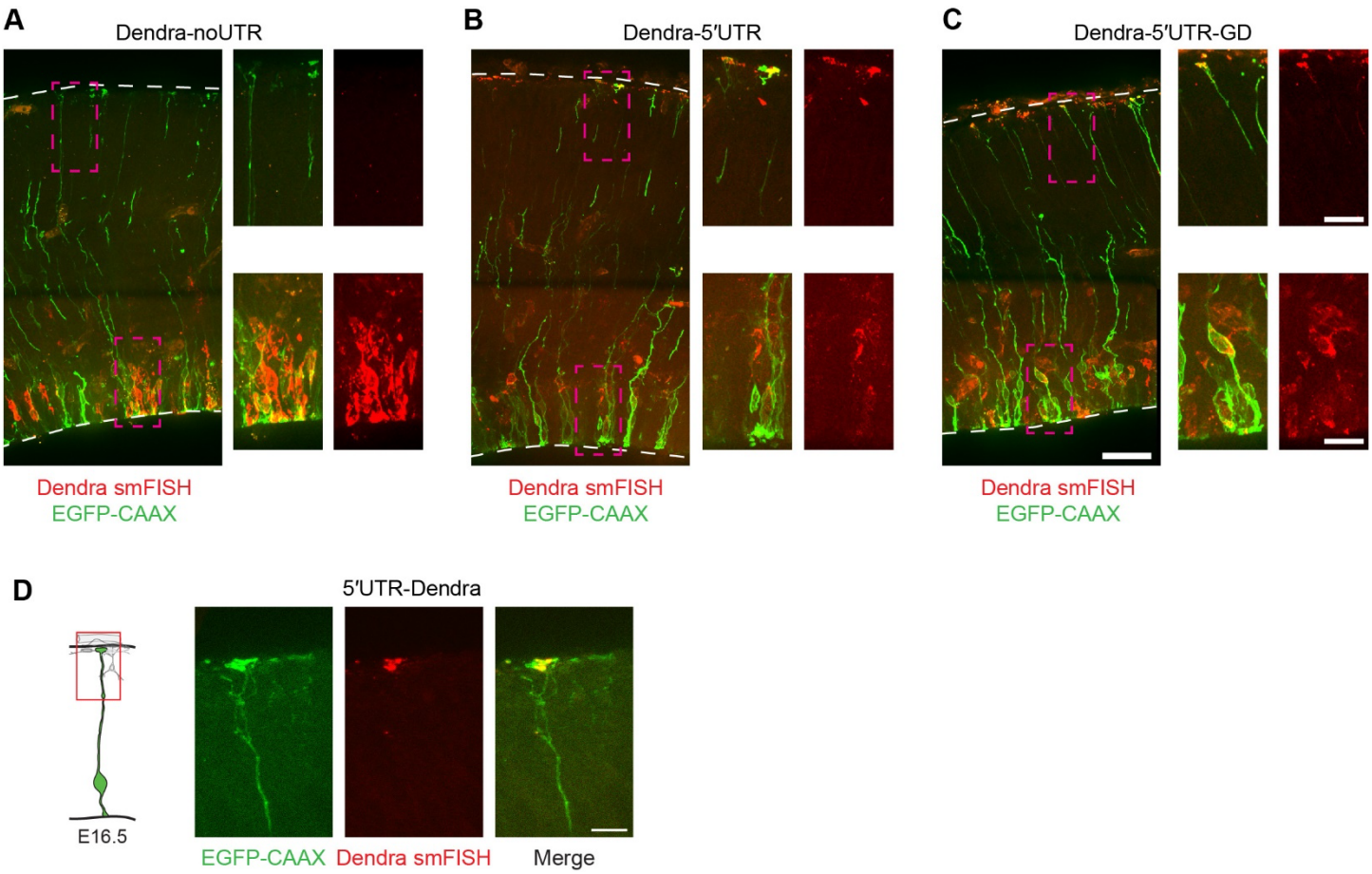

Figure S7. Localization of *Arhgap11a localization reporter* mRNAs to RGC basal endfeet and processes relies on a 5′UTR element,

Related to Figure 6.

(A-C) Single-molecule fluorescent *in situ* hybridization against *Dendra* (red) in E16.5 brains, electroporated one day earlier. This shows that *Dendra* reporter mRNAs including *Arhgap11a* 5′UTR show endfoot localization.

(D) The induction of RGC endfoot localization by the *Arhgap11a* 5′UTR sequence is position independent. As in experiments described in (A-C), *Arhgap11a* 5′UTR was engineered in the 3′UTR of dendra reporters. No RNA localization difference was observed when the *Arhgap11a* 5′UTR was engineered into the 5′UTR of the dendra reporter mRNA (D).

UTR: untranslated region, GD: gap-deficient. Scale bars: A-C (large panels) and D: 50μm, A-C (high magnification images): 20 μm.

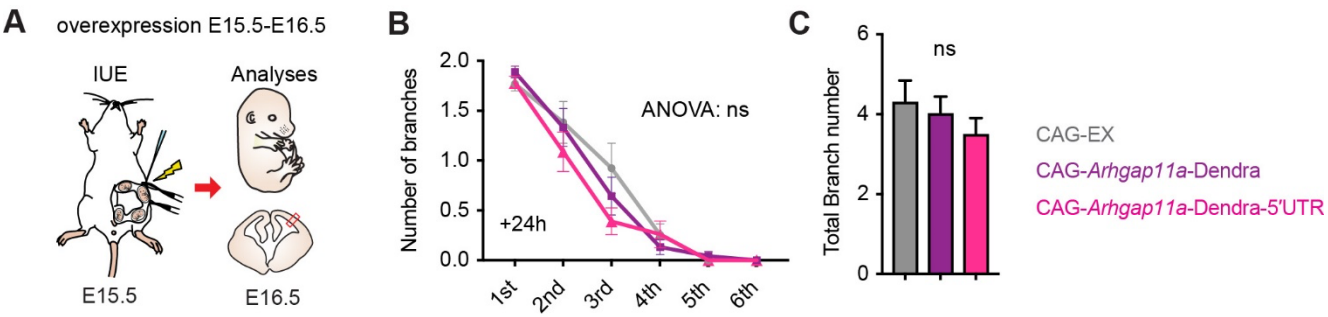

Figure S8. *Arhgap11a* overexpression does not impact RGC basal process complexity in the MZ, Related to Figure 7.

(A) Schematic overview of experiments to quantify the impact of acute *Arhgap11a* overexpression on basal process complexity in the MZ, two days after electroporation.

(B,C) *Arhgap11a* overexpression does not impact RGC basal process complexity. (CAG-EX: n=39 cells from 3 brains, 2 independent experiments, CAG-*Arhgap11a*-Dendra: n= 36 cells from 3 brains, 2 independent experiment, CAG-*Arhgap11a*-Dendra-5′UTR: n=45 cells from 4 brains, 2 independent experiments, two-way ANOVA).

IUE: *in utero* electroporation, UTR: untranslated region. ns: non-significant. Graphs show average values +/- SEM.